HHS Public Access

Author manuscript

*Magn Reson Med*. Author manuscript; available in PMC 2019 December 01.

Published in final edited form as:

*Magn Reson Med*. 2018 December ; 80(6): 2366–2373. doi:10.1002/mrm.27340.

# Prospective frequency correction using outer volume suppression-localized navigator for MR Spectroscopy and Spectroscopic Imaging

**Chu-Yu Lee**[1], **In-Young Choi**[1,2,3], and **Phil Lee**[1,3]

[1]Hoglund Brain Imaging Center, University of Kansas Medical Center, Kansas city, KS, USA

[2]Department of Neurology, University of Kansas Medical Center, Kansas city, KS, USA

[3]Department of Molecular & Integrative Physiology, University of Kansas Medical Center, Kansas city, KS, USA

## Abstract

**Purpose—**New frequency correction methods are required to achieve the accurate measurement of frequency drifts in magnetic resonance spectroscopy (MRS) and spectroscopic imaging (MRSI). We present a prospective frequency correction method with outer volume suppression (OVS)-based localization and selective water excitation for effective frequency correction with better signal-to-noise ratio (SNR) improvement compared to other techniques.

**Methods—**An OVS-localized navigator was developed to prospectively correct frequency drifts during MRS and MRSI measurements. The performance of the navigator was tested on the human brain and a solution phantom for frequency drifts induced by head motion or gradient heating by a preceding DWI experiment at 3 T.

**Results—**The OVS-localized navigator could accurately track motion-induced frequency drifts with a root-mean-square error (RMSE) of 0.5 Hz. The SNR of MRS signals was not affected by the use of the OVS-localized navigator when compared with and without the navigator ($p>0.05$). The frequency drifts induced by DWI experiments were 5.1±0.3 Hz/min during MRSI measurements on humans, resulting in increased spectral linewidth, significant bias in metabolite concentrations and significantly increased Cramér-Rao lower bounds (CRLB) ($p<0.05$). After prospective frequency corrections, the quality of MRSI was recovered to the level of those without any DWI induced frequency drifts, judged by the spectral linewidth, metabolite concentrations and CRLB.

**Conclusion—**The OVS-localized navigator demonstrated effective prospective frequency corrections for large frequency drifts (5 Hz/min) without introducing any saturation-induced SNR loss. These benefits can be particularly beneficial for the acquisition of MRS signals with long T1 and/or short TR, and spectral-editing.

Address correspondence to: Phil Lee, Ph.D., Hoglund Brain Imaging Center, Department of Molecular & Integrative Physiology, 3901 Rainbow Blvd, Mail Stop 1052, University of Kansas Medical Center, Kansas City, KS 66160, Phone: 913-588-0454, Fax: 913-588-9071, plee2@kumc.edu.

**Keywords**

magnetic resonance spectroscopy; magnetic resonance spectroscopic imaging; frequency drift; navigator; prospective frequency correction; outer volume suppression

## Introduction

Data acquisitions for single voxel spectroscopy (SVS) and magnetic resonance spectroscopic imaging (MRSI) require long scan times due to the low signal-to-noise ratio (SNR) with orders of magnitude lower concentrations of metabolites than water. The stability of the static magnetic field (B0) is important for the reliable acquisition of MR spectra. However, frequency drifts occur during scans even in advanced MR systems, and these drifts increase when high shim currents or rapidly switching gradients are applied (1). Frequency drifts can occur due to subject motion. The frequency drifts during SVS/MRSI measurements result in ineffective water suppression and errors in spatial localization. Frequency drifts also cause broad and distorted spectral lineshapes, reduced SNR, and quantification errors (2-10), especially when SVS/MRSI scans are performed after MRI scans with a high gradient duty cycle, e.g., FMRI and diffusion-weighted MRI (DWI).

In order to mitigate the effects of frequency drifts in SVS/MRSI, both retrospective and prospective frequency correction methods have been proposed (2-7,9-14). Retrospective frequency correction methods, however, cannot correct ineffective water suppression resulting from frequency drifts. Furthermore, retrospective frequency correction methods utilizing residual water signals or metabolite reference spectra (3,5,7,11-13) are not applicable to MRSI, where no reference water or metabolite signals are available due to phase encoding. In contrast, prospective frequency correction methods utilizing a navigator can be applied to SVS and MRSI, because the navigator is acquired separately from MRSI without phase encoding. A navigator in the prospective frequency correction methods is typically acquired in an interleaved manner, termed an interleaved reference scan (IRS) method (2,4,6,9,10,14). A small excitation flip angle is often used for the water navigator to reduce the saturation effects on MR spectra, acquired immediately after the navigator. The volume localization can be incorporated into the navigator acquisition (15), e.g., IRS-PRESS navigators (4,6), for the reduced spectral linewidth and the improved frequency drift estimation. Nevertheless, the IRS-PRESS navigators lead to the saturation-induced SNR loss even with a small excitation flip angle (10-20°) (4,6). The SNR loss becomes substantial when imperfect 180° refocusing pulses are used or when the T1 relaxation delay is short.

In this study, we propose a new prospective frequency correction method to obtain the localized navigator that effectively corrects motion- and gradient heating-induced frequency drifts, overcoming the aforementioned shortcomings of currently available methods. This proposed OVS-localized navigator method avoids perturbation of metabolite signals in MRS/MRSI, preventing any saturation-induced SNR loss.

## Methods

The proposed prospective frequency correction method utilizes a navigator with OVS localization (16,17) and selective water excitation for navigator acquisition (Fig. 1). The volume of interest (VOI) of OVS localization matched that of SVS or MRSI. Two-layer OVS bands were used to achieve a well-defined VOI with sharp transition. The first layer OVS bands were composed of six narrow saturation bands with 3 cm thickness and placed around the VOI. The second layer OVS bands with 10 cm thickness were placed outside the first layer of OVS bands with partial overlap. Following the OVS localization, a 90° frequency selective pulse was used to excite only water signals for the navigator. RF pulses used for OVS localization and selective water excitation were a high bandwidth frequency modulated pulse (HS1, pulse duration=4 ms, bandwidth=5 kHz) and an amplitude-modulated asymmetric pulse (duration=36 ms, bandwidth=127 Hz), respectively (18). The number of data points for the navigator was 512 and bandwidth was 2000 Hz. Water navigator signals ($FID_{nav}$, Fig. 1) were sent to the real-time reconstruction system. The receiver phase of each coil element of the 16-channel array coil was measured from the first time point of navigator signals and was subtracted from each navigator signal. After the phase correction, all navigator signals were summed together using SNR as a weighing factor, and zero-padded into 40960 points and Fourier transformed. The peak position of the water spectrum was used to measure the water frequency to update frequencies of RF pulses and the receiver for the remaining part of the sequence at each TR.

All experiments were performed on a 3T MR system (Skyra, Siemens AG, Erlangen, Germany) using a body transmit coil, a 16-channel head array receive coil and a vendor-supplied field mapping routine for shimming. Water suppression was achieved using a combination of variable power RF pulses with optimized relaxation delays (VAPOR) scheme (18). The OVS-localized navigator was incorporated into the semi-adiabatic localization by adiabatic selective refocusing (semi-LASER) (19) based SVS and MRSI sequences. For the SNR comparison, the PRESS-IRS navigator method with a navigator flip angle of 15° (4,6) was also implemented in the semi-LASER sequence.

OVS-localized and non-localized navigator signals were measured followed by the acquisition of unsuppressed water signals from the VOI without frequency corrections as a reference for accessing the precision of frequency tracking in a phantom containing acetate and lactate, and in a human. Frequency drifts were induced by gradient heating by a preceding 30-minute EPI-based DWI (TE/TR=105/4600 ms, bandwidth=1132 Hz/pixel, FOV=256 mm, base resolution=192, 2 b-values of 0 (1 average) and 1000 s/mm$^2$ (6 averages), 64 diffusion encoding directions) or by the subject's periodical head rotation (~10°) along the sagittal plane, i.e., nodding motion. The precision of the frequency tracking was quantified using RMSE. SVS parameters were: 512 data points, TE/TR=35/2500 ms, spectral width=2000 Hz, number of averages=64, voxel size=3×3×3 cm$^3$ and scan time=170 s.

The impact of OVS-localized navigator or PRESS-IRS navigator on SNR was estimated with normalized SNR changes, $(SNR–SNR_{no\text{-}nav})/SNR_{no\text{-}nav}$, in reference to SNR without any navigator. SNR was computed as a ratio of area under the acetate peak to the root mean

square noise. SNR was measured to access the saturation effects due to navigators at five TR values (1300, 1400, 1600, 1800, and 2000 ms) and each measurement was repeated five times. The SNR differences were assessed using a two-sample t-test.

Three MRSI scans were performed on 10 healthy subjects (two females and eight males; 36±9 years old, mean±SD): an initial MRSI scan before DWI without any frequency correction as a reference followed by two MRSI scans after DWI with and without frequency correction. MRSI parameters were: FOV=20×20 $cm^2$, slice thickness=2 cm, VOI=8×8 $cm^2$, 16×16 phase encoding, TE/TR=35/1600 ms, spectral width=2000 Hz and scan time for MRSI=304 s. The RMSE was used to quantify the short-term fluctuation of frequency drifts. All MR spectra were processed by applying zero-padding to 8192 points and a mild Gaussian apodization filter with 2.8 Hz line-broadening.

The spectral quality, including SNR and linewidth, metabolite concentrations, and CRLB were quantified using the Linear Combination of Model analysis (LCModel) (20), and were averaged over thirty-six voxels within the VOI of MRSI scans. In each subject, the mean values were compared between MRSI scans before and after DWI using the paired t-test with a significance level: $p<0.05$.

## Results

The frequency tracking precisions of our OVS-localized navigator and non-localized navigator were similar in correcting frequency drifts (RMSE=0.1 versus 0.1 Hz) induced by a preceding 30-minute DWI scan (Fig. 2A). However, only the OVS-localized navigator could track motion-induced frequency drifts in the human brain (RMSE=0.5 versus 4.4 Hz) (Fig. 2B).

The SNR of SVS with the OVS-localized navigator showed no significant difference compared to that without any navigator ($p>0.55$) (Fig. 3A). In contrast, the use of the IRS-PRESS navigator resulted in 9.7-13.7% lower SNR of SVS than without any navigator ($p < 0.0002$). The SNR loss was greater with shorter TRs (Fig. 3B).

In MRSI, linear frequency drifts induced by DWI were 5.1±0.3 Hz/min in humans and 5.2 Hz/min in a phantom determined by linear regression (Fig. 4A and 4B). The fluctuation of frequency drifts in humans showed no significant differences before and after DWI but was larger than the fluctuation in the phantom (0.4±0.1 Hz versus 0.1 Hz) (Fig. 4A and 4B). The DWI-induced frequency drifts resulted in broad and distorted lineshapes of MRSI spectra of both a phantom and the human brain (Fig. 4G and 4H). Spectral linewidth was increased from 4.0 Hz to 14.5 Hz in a phantom and increased from 5.6±0.6 Hz to 12.0±1.1 Hz in humans. In humans, the frequency drifts also resulted in significant biases of creatine and *myo*-inositol concentrations, and significantly increased CRLB of NAA, choline, *myo*-inositol, and glutamate+glutamine ($p<0.05$) (Table 1). With the frequency correction using the OVS-localized navigator, the linear frequency drift was reduced to 0.01 Hz/min in a phantom and 0.1±0.1 Hz/min in humans. The MR spectra acquired with the frequency correction showed comparable spectral quality compared with the spectra before DWI (Figs. 4E and 4F). The SNR of MRSI spectra in humans was 18.8±2.1 before DWI and was

18.1±2.0 and 19.7±2.6 after DWI (with and without correction). The spectral linewidth was reduced to 3.7 Hz in a phantom and 5.4±0.5 Hz in humans. The spectral linewidth, metabolite concentrations and CRLB showed no significant differences compared with those before DWI ($p>0.05$) (Table 1).

An addition of the OVS-localized navigator to 2D MRSI caused an increase of the specific absorption rate (SAR) value by 0.1-0.2 W/lb. The increase was approximately 7-13% of the SAR limit (1.5 W/lb) for head scans. At the minimum achievable TR of 1350 ms, the total SAR value with the added OVS-localized navigator was 0.7 W/lb and was below the SAR limit.

## Discussion

Our proposed frequency correction method with the OVS-localized navigator achieved accurate measurements of frequency drifts and effective frequency correction. The use of OVS localization and selective water excitation for the navigator ensured the narrow linewidth and maximum SNR of the navigator signals without any SNR penalty to metabolites by not perturbing the signals within the VOI. In contrast, IRS-PRESS navigator approaches could cause SNR loss of 10% or greater even with low flip angle excitation (10-20°), especially when short TR was used. The SNR loss with the IRS-PRESS navigator may be reduced by increasing TR or by decreasing the excitation flip angle of the navigator. However, these approaches may cause either increased scan time or reduced SNR of navigator signals.

Frequency drifts due to gradient heating after FMRI or DWI scans are much greater (1,2,6,21,22) than those due to system instability, <0.2 Hz/min on a 3T scanner (4). Our results show that when frequency drifts are large, frequency corrections at each TR are required to maintain accurate spatial encoding, spectral quality and effective water and lipid suppression. The consistent spectral alignment during the data acquisition is particularly important for MRSI with its prolonged scan time. Previously, navigator-based frequency correction methods have been proposed to correct frequency drifts in MRSI using non-localized water signals (9,10,14). However, some of these retrospective methods, where the frequency drifts at each TR are corrected using post-processing routines, provide only partial corrections for the effect of frequency drifts. For example, compromised water or lipid suppression efficiency due to frequency drifts cannot be corrected. Furthermore, non-localized navigators failed to track the motion-induced frequency drifts (Fig. 2). In contrast, the prospective frequency correction method using the OVS-localized navigator can effectively prevent the deleterious effect of large frequency drifts resulting from gradient heating and subject motion by acquiring each phase-encoded data with the correct frequency setting.

Accurate frequency setting is especially important for spectral-editing, which critically depends on the accuracy of frequency selective editing pulses with generally a very narrow bandwidth. The effects of inaccurate frequency setting due to frequency drifts during spectral editing are partial loss of edited signals or signal contamination from interfering signals. Most of the current spectral-editing utilizes retrospective frequency correction

methods (21,23-25). Only a recent study utilized a prospective frequency correction for GABA editing using an interleaved water referencing method, which corrects the frequency every 20 TR using a reference water signal (22). However, the interleaved water reference method may not effectively compensate large frequency drifts, e.g., ~5 Hz/min. For example, when the B0 frequency drift is 5.1 Hz/min and TR 4 s, the estimated frequency drifts are up to 6.8 Hz and 0.3 Hz for the interleaved water reference method and the current prospective frequency correction method, respectively. The frequency drift of 6.8 Hz is significant in GABA editing because interference from macromolecule signals to edited GABA signals can vary significantly with frequency drifts. Thus, the proposed prospective frequency correction method could enhance editing accuracy even large B0 frequency drifts occur during the scan.

Gradient heating-induced frequency drifts are approximated to vary linearly over time, whereas motion-induced frequency drifts, such as respiration, can exhibit short-term fluctuations in frequency (Figs. 4A and 4B) (2). In our study, the maximal fluctuation during MRSI was 1.2±0.8 Hz across human subjects and is comparable with the previously reported fluctuation in humans (~0.8 Hz) using a non-localized navigator (2). The fluctuations of frequency drifts can potentially be corrected using the OVS-localized navigator. However, the OVS-localized navigator can only correct for slow frequency drifts occurring between TRs. Furthermore, the precision of the frequency correction is limited by the scanner software, which only allows the modification using integers (26).

While we observed an increased signal peak and improved linewidth of the spectra with the frequency correction (Fig. 4), both SNRs with and without the frequency correction showed only ~5% percent changes in reference to SNR before DWI. Because the spectra of humans were influenced by both motion- and gradient heating-induced frequency drifts, it is unclear which frequency drifts mainly contribute to the changes of SNR. SNR in LCModel is computed as the signal peak subtracted by the baseline and divided by the fitting residuals (20). Therefore, the discrepancy may arise from inaccurate basis sets in conjunction with distorted broad line shapes (Fig. 4H) that could artificially reduce LCModel fit residuals.

Gradient heating-induced frequency drifts can be considered as spatially invariant changes in the B0 field with minimal effects on B0 inhomogeneity (1). However, when subject motion is present, frequency drifts within the VOI are spatially dependent (27) and can only be tracked using a VOI localized navigator. Furthermore, because the B0 field is disturbed, the system frequency correction alone is not sufficient. When head motion is present, additional adjustments such as the VOI position and first- and second-order shim currents will further improve spectral quality (11-13,26-31).

The water frequency of the navigator can be measured using time-domain phase fitting (2,10) or frequency-domain peak detection methods (2,6). These two methods have been shown to have similar accuracies to detect system instability-induced frequency drifts on a phantom (2). In the time-domain phase fitting method, frequency drifts are assumed to correspond to a linearly varying phase with time. However, motion-induced frequency drifts possibly result in non-linear phase evolution with time (32) and cannot effectively be

detected by the time-domain phase fitting method. Therefore, this study used the frequency-domain peak detection method to track frequency drifts.

The impact of the navigators on SNR was assessed using acetate in the phantom (Fig. 3). The T1 relaxation time of acetate was 3500 ms, measured using the saturation recovery sequence, and is longer than that of metabolites in the human brain, 1000–1500 ms (33). To reduce the long T1 relaxation-induced saturation effects, the impact of the navigators on SNR was estimated with normalized SNR changes. Because the SNRs with and without navigators are influenced by the T1 relaxation times, the normalized SNR changes only have a small dependence on the T1 relaxation times for a given TR, e.g., 1–2 % differences using a simulation.

Metabolite quantification typically requires additional unsuppressed water reference scans. For MRSI with a longer duration of the water reference scan, prospective frequency correction is necessary for accurate metabolite quantifications. However, the OVS-localized navigator with a 90° water excitation pulse can introduce saturations of water signals. Therefore, the flip angle of the water excitation pulse needs to be reduced to <10° to minimize the saturation effect on water signals.

The OVS-localized navigator required approximately 375 ms: OVS localization (77 ms), water excitation (42 ms), and navigator data acquisition (256 ms), which was similar to that for the IRS-PRESS navigator (~307 ms). This required time could be shortened by incorporating the OVS navigator into the VAPOR scheme (18).

The non-localized or slab-localized navigators with a 1° flip angle (2,9,10,14) are simple to implement and require less time with a negligible SNR loss. They can be applied to correct frequency drifts for MRSI with a whole-brain coverage or a thin slab VOI. However, those simple navigators may only provide limited or suboptimal precision to track and correct motion-induced frequency drifts when VOI selection is desirable for reducing subcutaneous lipid contamination (Fig. 2). Thus, in these cases, volume-localized navigators are necessary to compensate frequency drifts.

In conclusion, the proposed prospective frequency correction method using the OVS-localized navigator provides an effective real-time frequency correction with no SNR loss in the presence of large frequency drifts. In addition, the proposed method with no saturation-induced SNR loss can be especially beneficial for measurements of metabolites with a long T1 relaxation time and measurements that require short TR to reduce scan time in high-resolution MRSI with many phase encoding steps.

## References

1. Foerster BU, Tomasi D, Caparelli EC. Magnetic field shift due to mechanical vibration in functional magnetic resonance imaging. Magn Reson Med. 2005; 54(5):1261–1267. [PubMed: 16215962]
2. Henry PG, van de Moortele PF, Giacomini E, Nauerth A, Bloch G. Field-frequency locked in vivo proton MRS on a whole-body spectrometer. Magn Reson Med. 1999; 42(4):636–642. [PubMed: 10502751]

3. Helms G, Piringer A. Restoration of motion-related signal loss and line-shape deterioration of proton MR spectra using the residual water as intrinsic reference. Magn Reson Med. 2001; 46(2): 395–400. [PubMed: 11477645]
4. Thiel T, Czisch M, Elbel GK, Hennig J. Phase coherent averaging in magnetic resonance spectroscopy using interleaved navigator scans: compensation of motion artifacts and magnetic field instabilities. Magn Reson Med. 2002; 47(6):1077–1082. [PubMed: 12111954]
5. Ernst T, Li J. A novel phase and frequency navigator for proton magnetic resonance spectroscopy using water-suppression cycling. Magn Reson Med. 2011; 65(1):13–17. [PubMed: 20872862]
6. Lange T, Zaitsev M, Buechert M. Correction of frequency drifts induced by gradient heating in 1H spectra using interleaved reference spectroscopy. J Magn Reson Imaging. 2011; 33(3):748–754. [PubMed: 21563261]
7. Near J, Edden R, Evans CJ, Paquin R, Harris A, Jezzard P. Frequency and phase drift correction of magnetic resonance spectroscopy data by spectral registration in the time domain. Magn Reson Med. 2015; 73(1):44–50. [PubMed: 24436292]
8. Schmidt O, Widmaier S, Bunse M, Jung WI, Dietze GJ, Lutz O. Artifacts in CSI-measurements caused by the drift of the static magnetic field. Magma. 2000; 10(3):167–170. [PubMed: 10873207]
9. Ebel A, Maudsley AA. Detection and correction of frequency instabilities for volumetric 1H echo-planar spectroscopic imaging. Magn Reson Med. 2005; 53(2):465–469. [PubMed: 15678549]
10. Tal A, Gonen O. Localization errors in MR spectroscopic imaging due to the drift of the main magnetic field and their correction. Magn Reson Med. 2013; 70(4):895–904. [PubMed: 23165750]
11. Keating B, Deng W, Roddey JC, White N, Dale A, Stenger VA, Ernst T. Prospective motion correction for single-voxel 1H MR spectroscopy. Magn Reson Med. 2010; 64(3):672–679. [PubMed: 20806374]
12. Keating B, Ernst T. Real-time dynamic frequency and shim correction for single-voxel magnetic resonance spectroscopy. Magn Reson Med. 2012; 68(5):1339–1345. [PubMed: 22851160]
13. Zaitsev M, Speck O, Hennig J, Buchert M. Single-voxel MRS with prospective motion correction and retrospective frequency correction. NMR Biomed. 2010; 23(3):325–332. [PubMed: 20101605]
14. Zhu H, Edden RA, Ouwerkerk R, Barker PB. High resolution spectroscopic imaging of GABA at 3 Tesla. Magn Reson Med. 2011; 65(3):603–609. [PubMed: 21337399]
15. Bottomley PA. Spatial localization in NMR spectroscopy in vivo. Ann N Y Acad Sci. 1987; 508:333–348. [PubMed: 3326459]
16. Choi IY, Tkac I, Gruetter R. Single-shot, three-dimensional "non-echo" localization method for in vivo NMR spectroscopy. Magn Reson Med. 2000; 44(3):387–394. [PubMed: 10975890]
17. Henning A, Fuchs A, Murdoch JB, Boesiger P. Slice-selective FID acquisition, localized by outer volume suppression (FIDLOVS) for (1)H-MRSI of the human brain at 7 T with minimal signal loss. NMR Biomed. 2009; 22(7):683–696. [PubMed: 19259944]
18. Tkác I, Starcuk Z, Choi IY, Gruetter R. In vivo 1H NMR spectroscopy of rat brain at 1 ms echo time. Magn Reson Med. 1999; 41(4):649–656. [PubMed: 10332839]
19. Scheenen TW, Klomp DW, Wijnen JP, Heerschap A. Short echo time 1H-MRSI of the human brain at 3T with minimal chemical shift displacement errors using adiabatic refocusing pulses. Magn Reson Med. 2008; 59(1):1–6. [PubMed: 17969076]
20. Provencher SW. Automatic quantitation of localized in vivo 1H spectra with LCModel. NMR Biomed. 2001; 14(4):260–264. [PubMed: 11410943]
21. Harris AD, Glaubitz B, Near J, John Evans C, Puts NA, Schmidt-Wilcke T, Tegenthoff M, Barker PB, Edden RA. Impact of frequency drift on gamma-aminobutyric acid-edited MR spectroscopy. Magn Reson Med. 2014; 72(4):941–948. [PubMed: 24407931]
22. Edden RA, Oeltzschner G, Harris AD, Puts NA, Chan KL, Boer VO, Schar M, Barker PB. Prospective frequency correction for macromolecule-suppressed GABA editing at 3T. J Magn Reson Imaging. 2016; 44(6):1474–1482. [PubMed: 27239903]
23. Waddell KW, Avison MJ, Joers JM, Gore JC. A Practical Guide to Robust Detection of GABA in Human Brain by J-difference Spectroscopy at 3 Tesla Using a Standard Volume Coil. Magn Reson Imaging. 2007; 25(7):1032–1038. [PubMed: 17707165]

24. Bhattacharyya PK, Lowe MJ, Phillips MD. Spectral quality control in motion-corrupted single-voxel J-difference editing scans: an interleaved navigator approach. Magn Reson Med. 2007; 58(4):808–812. [PubMed: 17899594]
25. Evans CJ, Puts NA, Robson SE, Boy F, McGonigle DJ, Sumner P, Singh KD, Edden RA. Subtraction artifacts and frequency (mis-)alignment in J-difference GABA editing. J Magn Reson Imaging. 2013; 38(4):970–975. [PubMed: 23188759]
26. Bogner W, Gagoski B, Hess AT, Bhat H, Tisdall MD, van der Kouwe AJ, Strasser B, Marjanska M, Trattnig S, Grant E, Rosen B, Andronesi OC. 3D GABA imaging with real-time motion correction, shim update and reacquisition of adiabatic spiral MRSI. Neuroimage. 2014; 103:290–302. [PubMed: 25255945]
27. Hess AT, Andronesi OC, Tisdall MD, Sorensen AG, van der Kouwe AJ, Meintjes EM. Real-time motion and B0 correction for localized adiabatic selective refocusing (LASER) MRSI using echo planar imaging volumetric navigators. NMR Biomed. 2012; 25(2):347–358. [PubMed: 21796711]
28. Hess AT, Tisdall MD, Andronesi OC, Meintjes EM, van der Kouwe AJ. Real-time motion and B0 corrected single voxel spectroscopy using volumetric navigators. Magn Reson Med. 2011; 66(2): 314–323. [PubMed: 21381101]
29. Bogner W, Hess AT, Gagoski B, Tisdall MD, van der Kouwe AJ, Trattnig S, Rosen B, Andronesi OC. Real-time motion- and B0-correction for LASER-localized spiral-accelerated 3D-MRSI of the brain at 3T. Neuroimage. 2014; 88:22–31. [PubMed: 24201013]
30. Saleh MG, Alhamud A, Near J, van der Kouwe AJ, Meintjes EM. Volumetric navigated MEGA-SPECIAL for real-time motion and shim corrected GABA editing. NMR Biomed. 2016; 29(3): 248–255. [PubMed: 26663075]
31. Hess AT, Jacobson SW, Jacobson JL, Molteno CD, van der Kouwe AJ, Meintjes EM. A comparison of spectral quality in magnetic resonance spectroscopy data acquired with and without a novel EPI-navigated PRESS sequence in school-aged children with fetal alcohol spectrum disorders. Metab Brain Dis. 2014; 29(2):323–332. [PubMed: 24488204]
32. Posse S, Cuenod C, Lebihan D. Motion artifact compensation in H-1 spectroscopic imaging by signal tracking. J Magn Reson Ser B. 1993; 102:222.
33. Traber F, Block W, Lamerichs R, Gieseke J, Schild HH. 1H metabolite relaxation times at 3.0 tesla: Measurements of T1 and T2 values in normal brain and determination of regional differences in transverse relaxation. J Magn Reson Imaging. 2004; 19(5):537–545. [PubMed: 15112302]

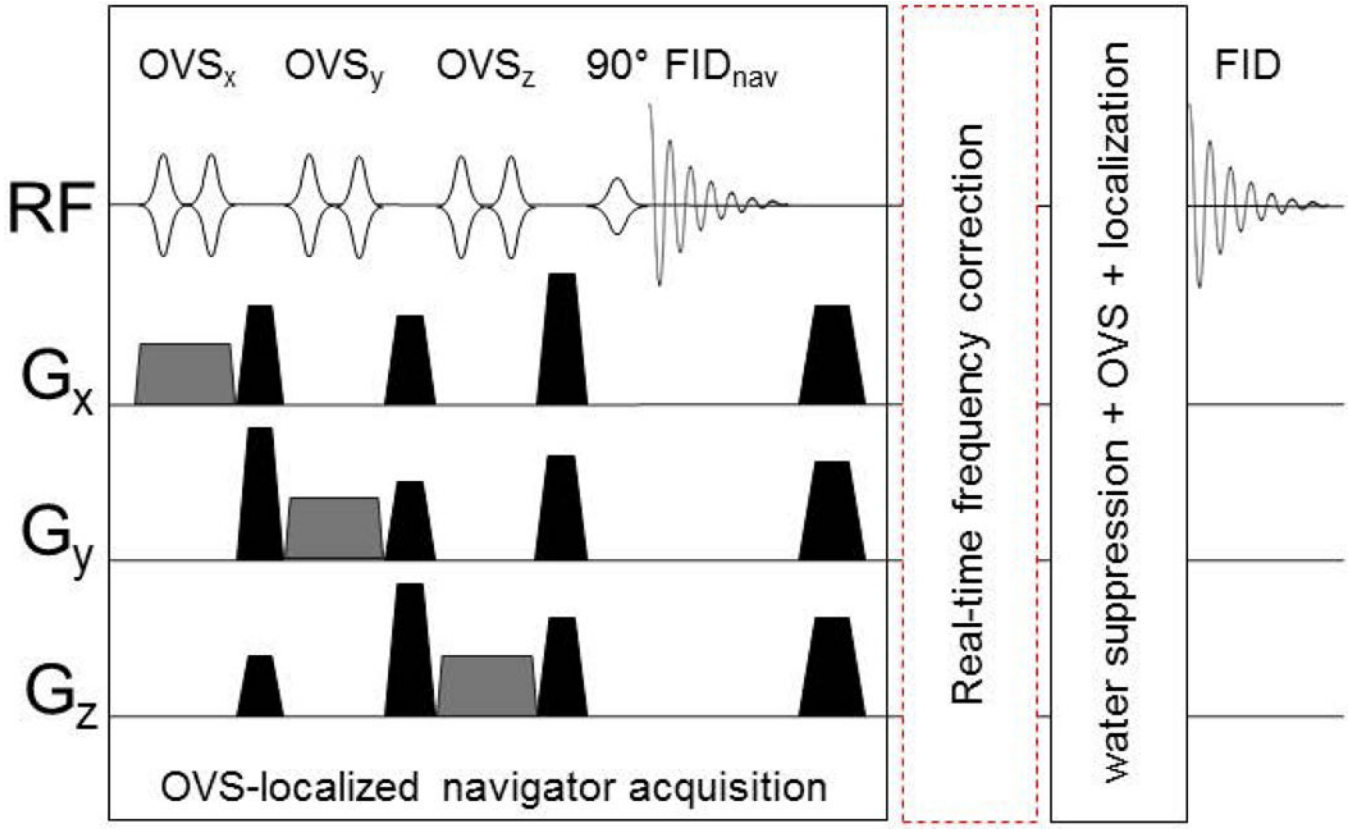


**Figure 1. Pulse sequence diagram of the proposed OVS-localized navigator method**

OVS localization in the OVS-localized navigator acquisition segment consisted of two layers of OVS bands in all three dimensions. Only one layer of OVS was shown for the simplicity of the figure. High bandwidth frequency modulated pulses (HS1, pulse width=4 ms, bandwidth=5 kHz) were used for OVS localization and an asymmetric amplitude modulated pulse (pulse width=36 ms, bandwidth=127 Hz) was used for selective water excitation. The frequency drift was measured at each TR from the navigator water signal in the real-time module of the scanner and used to update the frequencies of RF pulses in the following segment (water suppression+OVS+ localization) and the receiver prospectively at each TR.

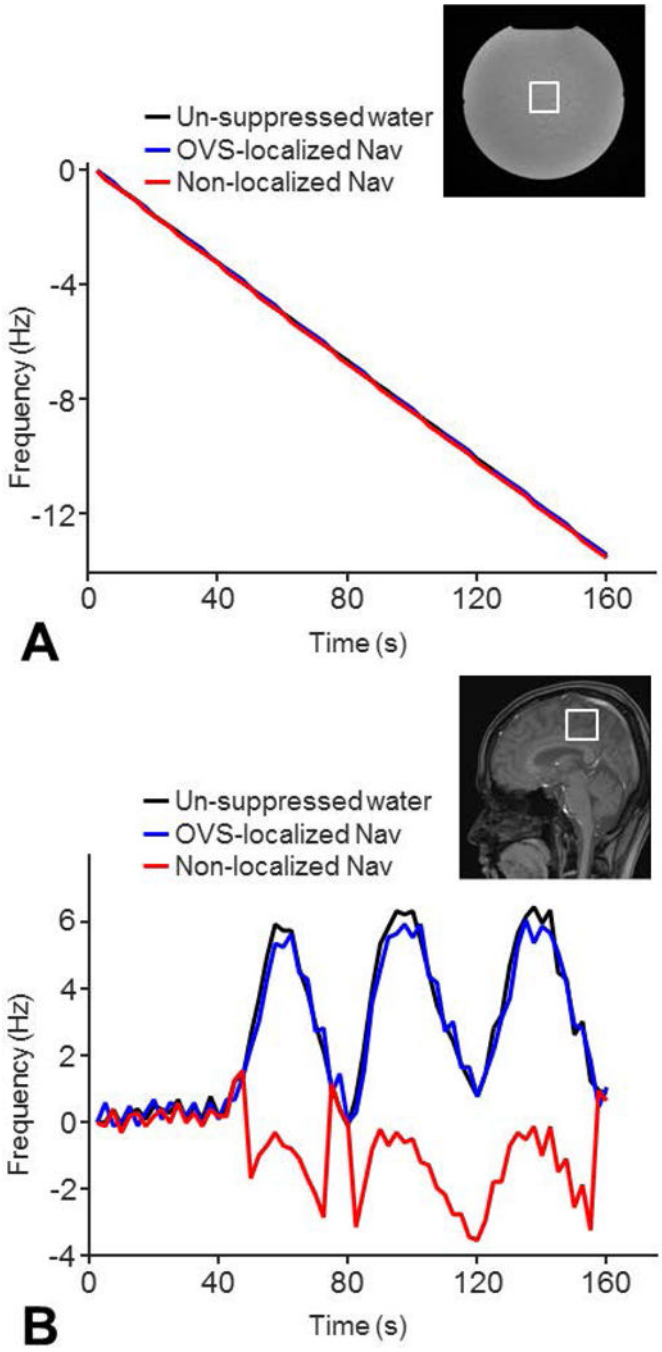


**Figure 2. Comparisons of frequency tracking precisions**

The frequency tracking precision of the OVS-localized navigator was compared to that of the non-localized navigator in a phantom with gradient heating-induced frequency drifts by a 30-min DWI experiment (**A**) and in a healthy volunteer with motion-induced frequency drifts (**B**). A healthy subject was instructed to rotate around 10° along the sagittal plane (nodding motion) periodically during the scan to simulate possible motion. The navigators and un-suppressed water signals were acquired in one single-voxel MRS sequence. The frequency drifts detected by the navigators were compared to those detected by the un-

suppressed water signals. The frequency tracking precisions of the navigators were quantified using RMSE.

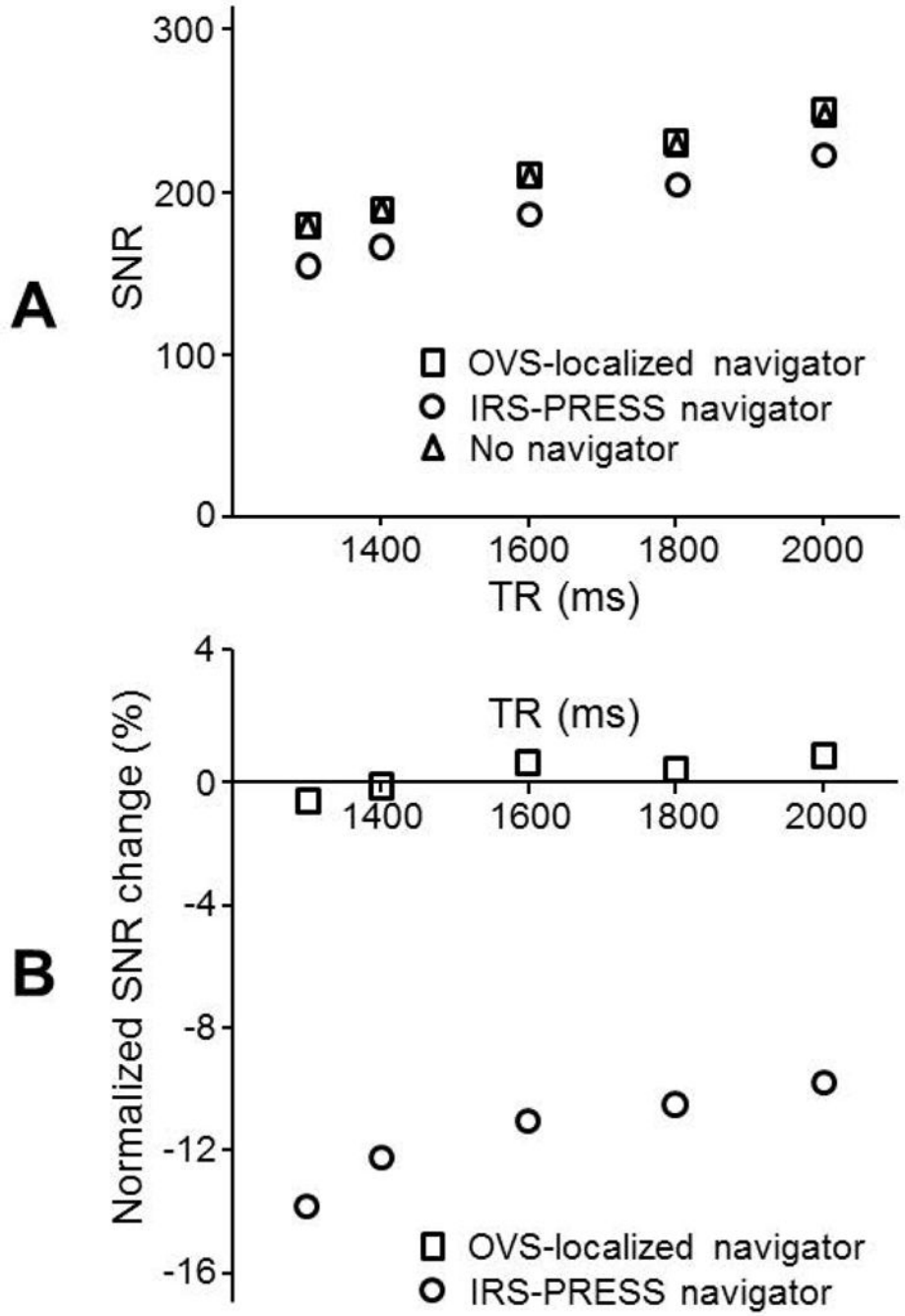


**Figure 3. SNR comparisons of two navigator methods at various TR**

(**A**) SNR of MR spectra with the OVS-localized navigator was compared to that with the PRESS-IRS navigator using SVS measurements on a solution phantom containing acetate and lactate. SNR was computed as a ratio of area under the acetate peak to the root mean square noise from a solution phantom containing of acetate and lactate. SVS parameters were: number of data points=512, BW=2000 Hz, number of averages=42, voxel size=3×3×3 $cm^3$, and TE=35 ms. (**B**) Normalized SNR changes, $(SNR–SNR_{no\text{-}nav})/SNR_{no\text{-}nav}$, were

calculated in reference to SNR without any navigator to compare the impact of a navigator addition in the two methods.

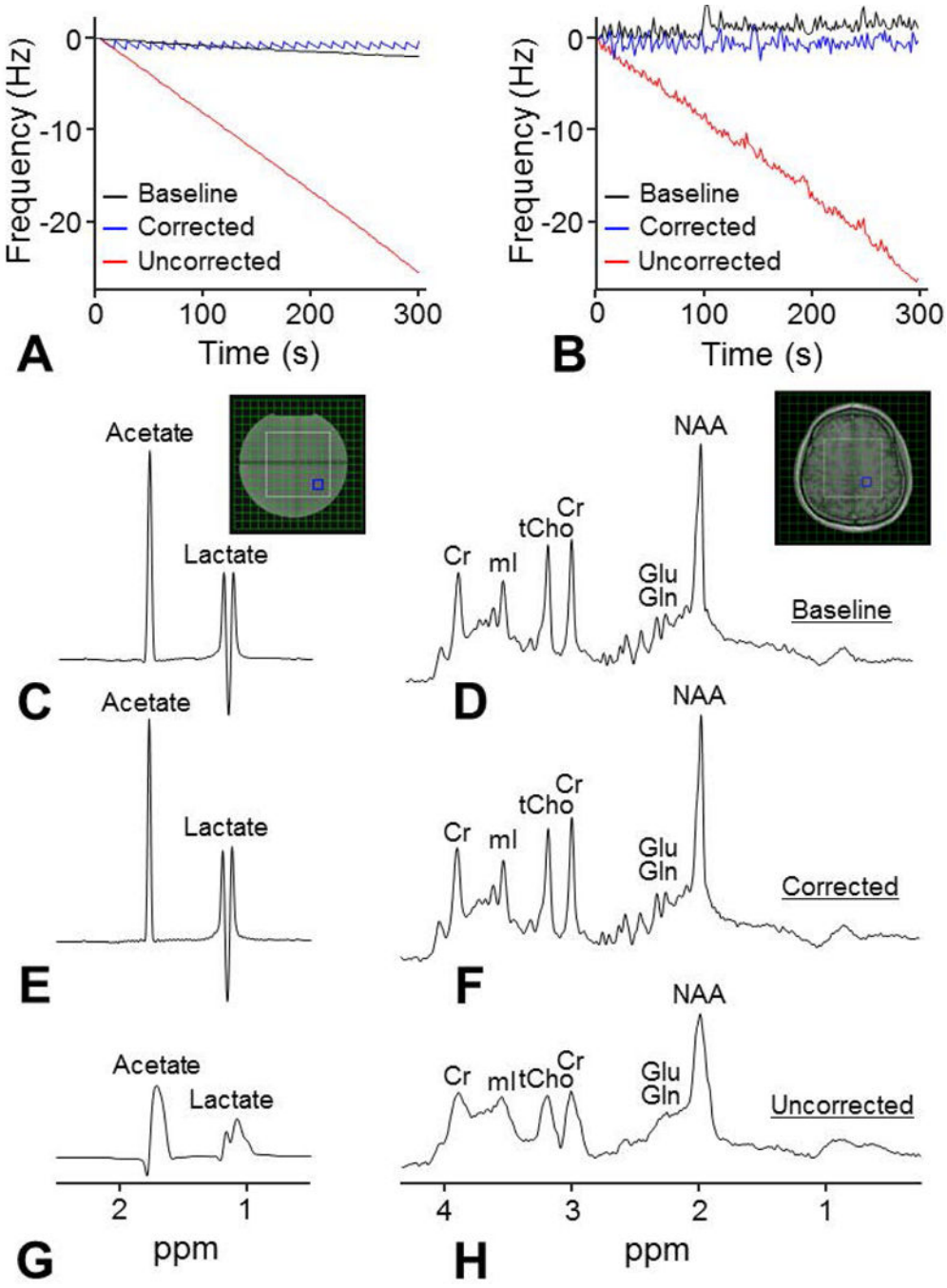


**Figure 4. Frequency drift correction in MRSI using the OVS-localized navigator method**

MRSI measurements were performed in the presence of gradient heating-induced frequency drifts on a phantom (**A**) and on a healthy volunteer (**B**) using the OVS-localized navigator. Frequency drifts following a 30-min DWI experiment were 5.2 Hz/min in the phantom and 5.1 Hz/min in the human brain. MRSI data were acquired using a semi-LASER sequence before the DWI experiment (baseline) (**C** and **D**) and after the DWI experiment with (**E** and **F**) and without (**G** and **H**) the prospective frequency correction. The OVS-localized navigator was acquired in all MRSI scans to monitor the frequency drifts. After the DWI

experiment, the spectra with the prospective frequency correction were comparable compared with the baseline spectra, while significant spectral broadening and distortion were visible from the spectra without the prospective frequency correction.

**Table 1**

Percentage changes in metabolite concentrations and the Cramér-Rao lower bounds (CRLB) after the DWI experiment with and without the prospective frequency correction. Percentage changes were computed in reference to the measurements before the DWI experiment and were the average across ten (*) indicates $p<0.05$ using a paired t-test.

| | Percent change in concentration (CRLB) | | | | |
|---|---|---|---|---|---|
| | **NAA** | **Cr** | **Cho** | **mI** | **Glu+Gln** |
| w/o corr | 1.9 (46.6*) | 9.2*(4.8) | −1.0 (24.4*) | 9.2*(13.2*) | 4.7 (12.4*) |
| w corr | −2.0 (2.2) | 0.3 (3.0) | 1.0 (2.3) | 1.7 (1.9) | 1.7 (0.6) |